Model Predictive Control Using MISO Approach for Drug Co-administration in Anesthesia

A. Pawłowski[1], **M. Schiavo**[2], **N. Latronico** [3], **M. Paltenghi**[4], **A. Visioli**[1]

[1]*Dipartimento di Ingegneria Meccanica e Industriale, University of Brescia, Brescia, Italy*
andrzej.pawlowski@unibs.it, antonio.visioli@unibs.it

[2]*Dipartimento di Ingegneria dell'Informazione, University of Brescia, Brescia, Italy*
schiavo003@unibs.it

[3]*Department of Surgery, Radiology, and Public Health, University of Brescia, Italy*
nicola.latronico@unibs.it

[4]*Spedali Civili di Brescia, Brescia, Italy*
massimiliano.paltenghi@asst-spedalicivili.it

This is the pre-print version of the following article: Model Predictive Control Using MISO Approach for Drug Co-administration in Anesthesi, which has been published in final form at https://doi.org/10.1016/j.jprocont.2022.07.007.

Abstract: In this paper, a model predictive control system for the depth of hypnosis is proposed and analyzed. This approach considers simultaneous co-administration of the hypnotic and analgesic drugs and their effect on the Bispectral Index Scale (BIS). The control scheme uses the nonlinear multiple-input single-output (MISO) model to predict the remifentanil influence over the propofol hypnotic effect. Then, it exploits a generalized model predictive control algorithm and a ratio between the two drugs in order to provide the optimal dosage for the desired BIS level, taking into account the typical constraints of the process. The proposed approach has been extensively tested in simulation, using a set of patients described by realistic nonlinear pharmacokinetic/pharmacodynamic models, which are representative of a wide population. Additionally, an exhaustive robustness evaluation considering inter- and intra-patient variability has been included, which demonstrates the effectiveness of the analyzed control structure.

1. Introduction

In general anesthesia it is necessary to achieve the desired patient state, considering that depth of hypnosis (DoH), analgesia and muscle relaxation must meet the requirements of the planned surgical intervention. The traditional approach is based on the anaesthesiologists, who take advantage of their knowledge and experience to adjust manually the drugs dosage basing on patient's vital signs as a feedback information. The anesthesia process is under continuous development with the aim of improving safety and efficacy. In this context, automatic control systems are seen as a potential technological progress in the operating rooms [1–5].

From a clinical practice standpoint, hypnosis and analgesia are always required in general anesthesia as the lack of one of these components produces serious intra-operative and post-operative complications. In total intravenous anesthesia, which is exclusively considered in this paper, propofol and remifentanil are commonly used as hypnotic and analgesic drugs, respectively. The neuromuscular blockade can be treated as a separate issue. Indeed, paralysis is not always required in general anesthesia. It is necessary only for specific types of surgery (e.g. abdominal surgery) and to facilitate particular procedures (e.g. intubation). Moreover, the drugs used for the neuromuscular blockade do not interact significantly with the analgesic or hypnotic drugs [6–8]. In total intravenous anesthesia, control systems have mainly focused on DoH, due to availability of its measure (e.g. Bispectral Index Scale [Medtronic], Entropy [GE Healthcare] or NeuroSense [Neuro Wave Systems]) which permits feedback control. There are several control structures where propofol is used as the hypnotic drug and the BIS signal is the process variable [9–11]. However, the single-input-single-output (SISO) control system for the DoH by itself does

not give a full support to the anaesthesiologist [2, 11]. In fact, hypnosis and analgesia should be addressed simultaneously due to the synergistic effect between the propofol and the analgesic drug remifentanil. The desirable control architecture should have a multiple-input-multiple-output (MIMO) structure, in order to handle the mutual interaction between control variables (the drugs dosage) and controlled variables (DoH and analgesia) [12–15].

A compromise between the MIMO and the SISO approaches is a multiple-input-single-output (MISO) process structure, where the BIS (or another measure for the DoH) is the only controlled variable and the infusion of propofol and remifentanil are the manipulated variables. Their mutual interaction has to be taken into account because, when used simultaneously, the resulting effect of each drug is bigger than expected with respect to when each drug is infused individually. In fact, in [16–18] it was shown that this interaction is especially important when the propofol is administrated in boluses (in the induction phase of the anaesthesia) and in presence of the surgical stimuli in the maintenance phase. The effect that this interaction has on DoH has also been well described in a pharmacokinetic/pharmacodynamic (PK/PD) model using the generalization of the Hill function to a surface. Among different parametrization techniques for the interaction surface model, the most accepted in the literature has been developed in [18–23]. This model shows that the same BIS can be obtained with different combinations of propofol and remifentanil dosages. This needs to be taken into account when designing the automatic control system.

Control architectures for the MISO case in anaesthesia process have been analyzed in several works over the last few years [24–33]. The effectiveness of classical proportional-integral-derivative (PID) control techniques has been shown in [27, 29, 30]. Then, sustainability and safety aspects for feedback control have been analyzed in [26, 32], where it has been demonstrated that there are clear advantages in the application of automatic controllers. A mid-ranging control technique exploiting the faster dynamics of remifentanil has been proposed in [33], where simulation results showed a satisfactory performance for the considered virtual patients. A robust control system considering additional compensator and base-line remifentanil dosage under habituating control technique has been analyzed in [24] focusing on the DoH, represented by a WAV_{CNS} signal. Moreover, some closed-loop control systems with extended logic, like Bayesian and multi-centre systems, have been analyzed in [25, 28] looking for the controller adaptability and focusing on the strong variability of the DoH process.

The availability of the interaction model between the propofol and the remifentanil has also stimulated the development of model predictive control (MPC) systems [34–37] for the MISO case. In this context, the predictive controller is built using a linearized interaction model for propofol and remifentanil, with the aim of keeping the desired level of the DoH [34]. The analgesic drug infusion rate is adapted to the propofol dosage and the ratio is kept constant. Another example where a habituating control technique and is reformulated for the DoH in anaesthesia control task taking into account the effect of remifentanil was shown in [35]. In this control system, a reference signal is established for the infusion rate of remifentanil and this is modified by the controller according to the changes in propofol dosage. In this way, the hypnosis is the main controlled variable and analgesia is adapted to the changes in the hypnosis feedback loop. Moreover, nonlinear MPC techniques have been analyzed in [36, 37], where conceptual developments are proposed for anaesthesia control.

These works show that MPC controllers can address relevant issues that concern process constraints and prediction capability of synergistic effect of drugs interaction. However, on the one hand, their applicability is limited by the strong variability of the process, namely, inter- and intra-patient variability. On the other hand, due to nonlinear process characteristics, resulting control systems are complex and rarely robust enough to be exploited at the operating room. Additionally, there exists many types of medical interventions with different requirements during the anaesthesia procedure, which makes difficult to develop one control system that is suitable for all situations. Furthermore, a personalized controller design based on patient model can significantly improve the control performance. This approach was previously investigated in a context of diabetes control system using a MPC-based techniques proving the effectiveness of this methodology [38, 39]. All aforementioned questions stimulate the development of new control systems based on MPC techniques.

In this paper, we propose an MPC system for the MISO process where the nonlinear propofol-remifentanil interaction model on the BIS is exploited [18]. The method suitably generalizes the idea proposed in [40], where the propofol is the only used drug. The control system employs an external predictor to compute the inverse of the static nonlinear element (represented as the Hill surface) of the drug interaction model, which enables the application of the linear MPC technique. In fact, the considered patient model has a Wiener structure, where the PK element is linear and the PD part has a nonlinear behaviour. The linear component is computed individually for each patient, while the nonlinear element is always the same since it cannot be obtained for each individual. The feedback controller is designed considering the linear term of the personalized patient model. In particular, a generalized predictive control (GPC) algorithm is used as feedback controller, which considers the effect of remifentanil over the propofol. Therefore, it is able to handle the synergistic effect of both drugs in the computation of the control signal for the DoH. The dosage of the two drugs is established by fixing a ratio between them [29]. The external predictor architecture is completed with the low-pass filter in the feedback loop. The tuning of the

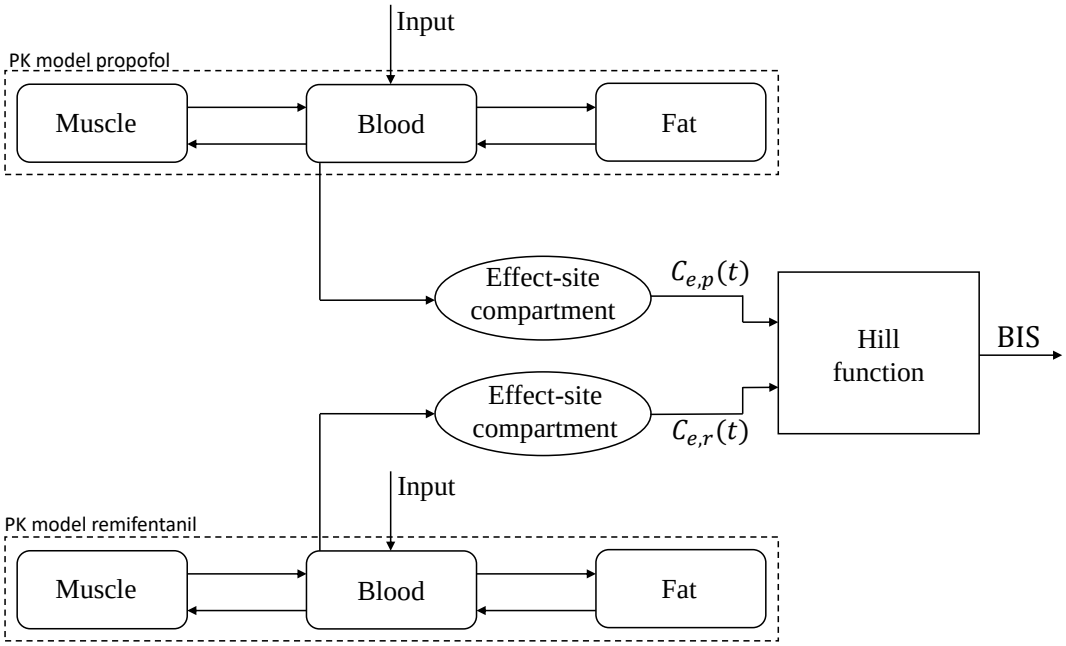

Fig. 1: A diagram interpretation of a PK/PD model of the patient using a three compartmental approach.

controller is performed by means of a genetic algorithm addressing separate requirements for the induction and the maintenance stages. Finally, the proposed control system is evaluated using a Monte Carlo technique for inter- and intra-patient variability using a wide distribution of patients population.

The remainder of paper is as follows. In Section 2, the propofol-remifentanil PK/PD interaction model exploited in the proposed control architecture is briefly reviewed. Section 3 is devoted to the analysis of the proposed control structure for the depth of hypnosis. Additionally, the GPC algorithm description and the tuning procedure are also provided there. Next, in Section 4, the proposed control system is tested for induction and maintenance stages using the simulation study. Moreover, exhaustive intra- and inter-patient variability tests using Monte Carlo analysis are also included. Lastly, conclusions are provided in Section 5.

2. Interaction model for drug co-administration

It is well known that co-administration of analgesic drugs like remifentanil with propofol have a synergistic effect that affects the hypnosis level of the patient [16,18,41]. Therefore, it is fundamental to have compartmental models exploiting PK/PD concepts that characterize the patient's response to these drugs. From a practical standpoint, the synergistic action results into a reduction of the amount of dosed propofol that is required to reach a desired level of hypnosis (measured by the BIS) if remifentanil is added [42]. From a model-based control system point of view, it is required to build the MISO model that has the propofolol infusion rate $u_p(t)$ and the remifentanil infusion rate $u_r(t)$ as inputs (control variables) and the DoH, measured through the BIS signal, as output (controlled variable).

2.1. Patient model

For the DoH, the relationship between the used drugs is usually modeled through a MISO Wiener model representation. In this architecture (see Figure 1), two linear systems representing two separate PK/PD models are connected in parallel and coupled with a static nonlinear function [17, 43, 44]. The distribution and elimination of the drug, considering the relation between drug administration and the plasmatic concentration in the patient body, is described by the pharmacokinetics. Instead, the pharmacodynamics represents the relation between the plasmatic concentration and resulting effect on site concentration. Moreover, in [16] it has been shown that propofol pharmacokinetics do not interact with the remifentanil action and absorption. The combined effect of the two drugs is considered in the pharmacodynamic part of the model, where a resulting Hill function gives the level of the DoH (represented by the BIS signal) taking into account the concentrations of used drugs.

A mammillary three-compartmental representation of model is frequently used to characterize the PK term of both drugs. Moreover, a homogeneous characteristic, like a uniform drug distribution, of the used model is assumed.

In this case, the infusion rate of the drug $u(t)$ is represented by the input of the model , while the plasmatic

concentration of the drug $C_p(t)$ is the output of the PK term. The resulting PK transfer function has the following form:

$$PK(s) = \frac{C_p(s)}{U(s)} = \frac{1}{V_1} \frac{(s+z_1)(s+z_2)}{(s+p_1)(s+p_2)(s+p_3)} \tag{1}$$

where the parameters p_1, p_2, p_3, z_1 and z_2 are related to the patient's physical characteristics (age, weight, height, gender) [17, 44, 45].

Then $C_p(t)$ (drug's plasmatic concentration) is the input of the PD term of the model. Its first part includes two linear first-order transfer functions corresponding to each drug. Each of them relates the plasmatic concentrations $C_p(t)$ to the effect-site concentrations $C_e(t)$. The linear part of PD model results therefore in the following general formulation:

$$\dot{C}_e(t) = k_{1e} C_p(t) - k_{e0} C_e(t), \tag{2}$$

where for propofol, k_{1e} has fixed value equal to 0.456 min^{-1} and it is equal to k_{e0}. For remifentanil, k_{1e} and k_{e0} are related to the patient's age:

$$k_{1e} = k_{0e} = 0.595 - 0.007(Age - 40). \tag{3}$$

Finally, the PD model is completed by a static nonlinear element, referred to as Hill function, which combines the effect-site concentrations of opioid and hypnotic drugs, giving the BIS value as

$$BIS(t) = E_0 - E_{max} \left(\frac{\left(\frac{Y_p(t) + Y_r(t)}{U_{50}(\phi)} \right)^{\gamma}}{1 + \left(\frac{Y_p(t) + Y_r(t)}{U_{50}(\phi)} \right)^{\gamma}} \right) \tag{4}$$

where:

- E_0 refers to the state of the patient, where no infusion is provided (initial state);
- $E_{max} - E_0$ is the maximum allowable effect;
- γ describes the gradient of the curve, characterizing the receptiveness of the patient to drugs;
- Y_p and Y_r are the propofol and remifentanil effect-site $C_{e,p}(t)$ and $C_{e,r}(t)$ concentrations (resulting from the linear model (2)), respectively, normalized with respect to $C_{e_{50},p}$ and $C_{e_{50},r}$. These are the propofol and remifentanil concentrations necessary to get half of the maximum effect over the DoH measure (BIS level), resulting in:

$$Y_p(t) = \frac{C_{e,p}(t)}{C_{e_{50},p}}, \quad Y_r(t) = \frac{C_{e,r}(t)}{C_{e_{50},r}}, \tag{5}$$

- $U_{50}(\phi)$ represents the power of two drugs at the ϕ co-administration ratio, expressed as the number of units related to the 50% of the maximum effect:

$$U_{50}(\phi) = 1 - \beta\phi + \beta\phi^2 \tag{6}$$

  where β is used to correlate the number of units associated with 50% of the drug maximum effect with the action of the drug and

$$\phi = \frac{Y_p(t)}{Y_p(t) + Y_r(t)}, \tag{7}$$

  expresses the power of the combination of drugs. An increased value of β results in a higher hypnotic effect because of the synergistic properties of drugs

The resulting interaction is super-additive. In this case, the combined effect of propofol and remifentanil is greater than the sum of the each one. The resulting BIS value is normalized in range 0 and 100, representing respectively, isoline and patient in fully awake state.

2.2. *Patients dataset*

The introduced PK/PD model also includes the dynamics of the BIS monitor, as previously shown in [45, 46]. Hence, it can be used to develop and evaluate the automatic control of the DoH by the coadministration of hypnotic and analgesic drugs. To this end, an already accepted set of PK/PD patient models, which are representative of a wide population, has been considered. The propofol-related parameters of the model are obtained from [9, 47, 48], while the variables related to remifentanil are randomly generated basing on the normal distribution of the

Id	Age	Height [cm]	Weight [kg]	Gender	$C_{e_{50},p}$	$C_{e_{50},r}$	γ	β	E_0	E_{max}
1	40	163	54	F	6.33	12.5	2.24	2.00	98.8	94.10
2	36	163	50	F	6.76	12.7	4.29	1.50	98.6	86.00
3	28	164	52	F	8.44	7.1	4.10	1.00	91.2	80.70
4	50	163	83	F	6.44	11.1	2.18	1.30	95.9	102.00
5	28	164	60	M	4.93	12.5	2.46	1.20	94.7	85.30
6	43	163	59	F	12.00	12.7	2.42	1.30	90.2	147.00
7	37	187	75	M	8.02	10.5	2.10	0.80	92.0	104.00
8	38	174	80	F	6.56	9.9	4.12	1.00	95.5	76.40
9	41	170	70	F	6.15	11.6	6.89	1.70	89.2	63.80
10	37	167	58	F	13.70	16.7	3.65	1.90	83.1	151.00
12	42	179	78	M	4.82	14.0	1.85	1.20	91.8	77.90
12	34	172	58	F	4.95	8.8	1.84	0.90	96.2	90.80
13	38	169	65	F	7.42	10.5	3.00	1.00	93.1	96.58

Table 1: Patient database for the propofol-remifentanil combined infusion models.

parameter values given in [49] to introduce inter-patient variability. The values for the considered population are presented in Table 1. The thirteenth individual is the average patient of the group, obtained by calculating for each available parameter its algebraic mean.

3. Control system

In this section, the design of the control system is described. First, the clinical requirements and the constraints for the DoH are presented. Secondly, the proposed MISO MPC architecture is presented. Finally, the tuning procedure for the control system is explained.

3.1. Control requirements

In the induction phase of the anesthesia, the goal of the coadministration control system is to bring the BIS value to the set-point value of 50 in a time interval smaller than 5 minutes (preferably in about 2 minutes), with a reduced undershoot. Values of BIS below 30 should be avoided, since they are correlated with the onset of burst suppression [50], which has been associated with postoperative delirium [51]. Then, during the maintenance phase, the BIS level should be maintained in the range between 40 and 60 as long as possible. Moreover, the control system must also be robust against the variability of the model, being able to deal with different physical characteristics (including estimation uncertainties) and health conditions of the patients.

An additional specification to be considered is the physical limitations of the actuators, that is, the saturation and slew rate limits of the used pumps (in our case Graseby 3400, Smiths Medical, London, UK). For this device, the lower saturation limit is set to 0 for two drugs, whereas the upper infusion limit for propofol is set to 6.67 mg/s (Diprivan 20 mg/ml) and for remifentanil to 16.67 μg/s (Ultiva 50 μg/s) [45]. Additionally, the pump slew rate limits, are 0.2 mg/s for the propofol and 0.4 μg/s for remifentanil, constraining the biggest allowed variation of the infusion rate from the previous sampling interval to the current one.

For the control system design, analysis and evaluation we set a fixed ratio of 2 between propofol and remifentanil dosage. Note that this ratio can vary as the type of surgical intervention changes. However, this value of the ratio is the most typical one as it is obtained by applying the infusion pattern proposed in [52]. Its goal is to achieve a balance between the propofol and remifentanil effect-site concentrations that ensures a 50% chance of not responding to surgical stimuli and the quickest return to consciousness after the end of infusions.

3.2. Control system architecture using MISO approach for drug coadministration

The introduced control system is a generalization and extension to the MISO case of the architecture presented in [40]. The main idea consists in the computation of the inverse of the nonlinear function present in the Wiener model and in the use of a linear GPC algorithm. The MISO Wiener model approach is used to consider the synergistic effect of the drug coadministration on the DoH represented by the BIS signal.

The control scheme is shown in Figure 2. The main objective is that the measured DoH level, shown as $BIS(t)$, follows the reference signal $\overline{BIS}(t)$. The patient model (see Section 2.1) has been conveniently reorganized into three blocks P_{prop}, P_{remif} and H. In this configuration the Wiener structure is maintained, as the first two elements

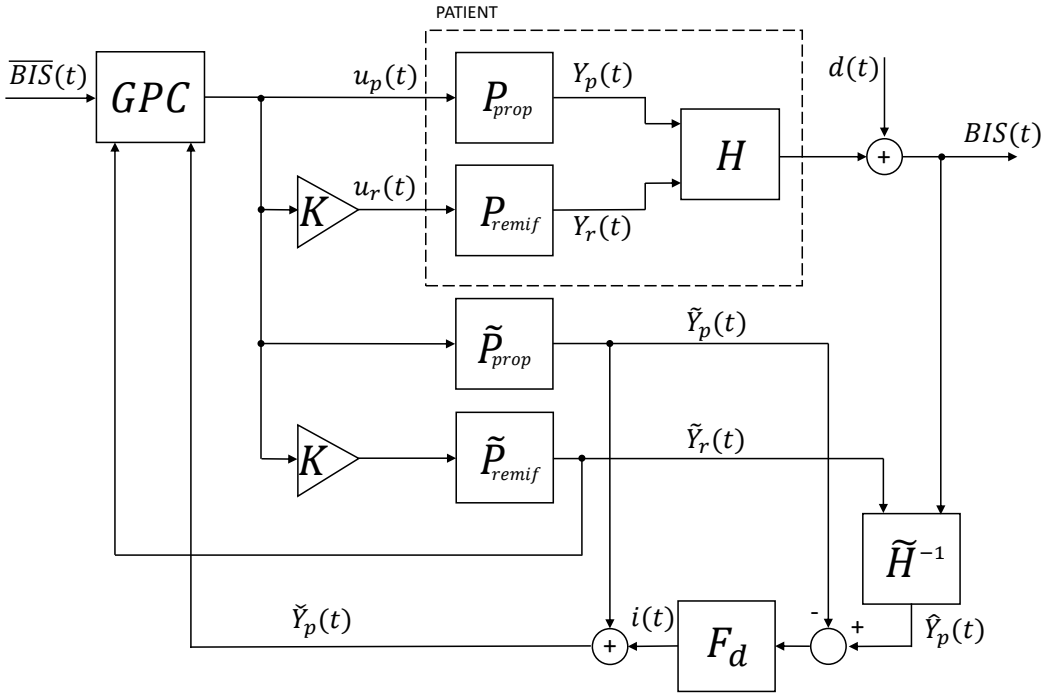

Fig. 2: The proposed control system for anesthesia using MISO approach for propofol-remifentanil coadministration.

represent the linear dynamics of the propofol and the remifentanil, respectively, and the H block represents the nonlinear Hill function. The main idea consists in using this model to construct an external predictor to estimate the patient state. The predictor blocks include the model of the linear dynamics $\tilde{P}_{prop}$ and $\tilde{P}_{remif}$ and the inverse of the nominal nonlinear function $\tilde{H}^{-1}$. The GPC block represents the feedback controller, K is the ratio between the co-administrated drugs and F_d is a low-pass filter. In this control architecture, the GPC controls directly $\tilde{Y}_p$, namely, the propofol concentration required to achieve the desired BIS value. This value can also be obtained from the process (in this case it is denoted as $\hat{Y}_p$) by using the $\tilde{H}^{-1}$ block that requires, as inputs, the actual BIS value and the remifentanil concentration $\tilde{Y}_r$ estimated by the predictor. Due to the unavoidable process/model mismatches, the resulting difference signal between $\hat{Y}_p$ and $\tilde{Y}_p$ is filtered by F_d in order to compensate for this difference in the feedback loop.

The introduced methodology requires a deeper analysis of the inverse nonlinear function block. The calculation of the inverse of the Hill function, which provides the value of $\hat{Y}_p$, requires the values of the BIS and of $\tilde{Y}_r$. The BIS value is provided by the DoH monitor, while $\tilde{Y}_r$ can be computed from the patient model (see (5)). To apply this methodology, Equation (4) needs to be rewritten as $Y_p(t) = f(BIS(t), Y_r(t))$. To obtain this structure, it is necessary to rewrite (4) using a third-order polynomial form, resulting in following equation:

$$Y_p^3 + bY_p^2 + cY_p + d = 0 \tag{8}$$

where:

$$b = 3Y_r - \left(\frac{E_0 - BIS}{E_{max} - E_0 + BIS}\right)^{1/\gamma}$$

$$c = 3Y_r^2 - 2Y_r\left(\frac{E_0 - BIS}{E_{max} - E_0 + BIS}\right)^{1/\gamma} + \beta Y_r\left(\frac{E_0 - BIS}{E_{max} - E_0 + BIS}\right)^{1/\gamma}$$

$$d = Y_r^3 - Y_r^2\left(\frac{E_0 - BIS}{E_{max} - E_0 + BIS}\right)^{1/\gamma}$$

Now, exploiting the current BIS signal measure and $\tilde{Y}_r(t)$ (which represents the estimated effect site concentration of remifentanil) it is possible to calculate $\hat{Y}_p(t)$, by solving (8), to finally obtain the inverse of the Hill function.

Once the inverse function is computed, its value from Equation (8) can be used to estimate the propofol concentration $\hat{Y}_p$. However, to integrate the effect of the remifentanil over the propofol, it is necessary to relate the desired propofol concentration (which is the reference signal for the GPC controller) to the remifentanil concentration and to the BIS desired value $\overline{BIS}(t)$. This is achieved by integrating the drugs co-administration effect into the $\tilde{Y}_p(t)$ value when computing the corresponding concentration for the BIS reference value. Thus, the calculation of the reference value (represented as $w(k)$ in the GPC structure, see Section 3.3) for the propofol concentration needs to take into account the value of Y_r. In the analyzed scheme the remifentanil dosage is related to the propofol infusion using a fixed gain K (as shown in simplified representation in Figure 3). Therefore, using basic properties of such a system, it is possible to obtain Y_r as an expression that depends on Y_p:

$$Y_p = G_p u_p \qquad\qquad Y_r = G_r u_r = G_r K u_p$$

From here, it is possible to obtain:

$$Y_r = G_p^{-1} G_r K Y_p \tag{9}$$

and from this, it is possible to obtain a difference equation:

$$Y_r(k) = b_0 Y_p(k) + \ldots + b_{n_b} Y_p(k - n_b) - a_0 Y_r(k-1) - \ldots - a_{n_a} Y_r(k - 1 - n_a) \tag{10}$$

where the coefficients a, b and the degrees n_a, n_b of the nominator and denominator are obtained from the $G_p^{-1} G_r K$ term.

At this point, Y_r in the equation (8) can be substituted with Y_r from equation (10). In this way, we obtain an expression where the propofol concentration is linked only to the desired level of DoH (the BIS setpoint value for the control system). Thus, we can determine an optimal reference signal for the propofol infusion that takes into account the effect of the remifentanil. This is possible thanks to the ratio block and to the exploitation of the propofol control signal values computed over the control horizon. The reference signal has slight variations at each sampling instant because the relation between Y_p and Y_r depends on the past values of Y_p and Y_r. To take into account this relationship, the reference $w(t)$ is computed at every sampling instant, using a receding horizon strategy. Thanks to the proposed architecture it possible to obtain MISO control system properties. However, the SISO model is considered for the GPC controller design.

At this stage, the advantages of the proposed control scheme can be provided. Under nominal conditions, when there are no uncertainties and modelling errors among the patient and the derived model, (i.e. $\tilde{P}_{prop} = P_{prop}$, $\tilde{P}_{remif} = P_{remif}$ and $\tilde{H} = H$) the analyzed scheme can be transformed to a linear syste, where the controller is focused on the linear element of the patient model. In such a scenario, $w(t)$ is obtained from $\overline{BIS}(t)$ by applying H^{-1}, which includes the effect site concentration of remifentanil. In this way the BIS is linked to the $C_{e,p}(t)$ value, which is the estimated propofol effect-site concentration the patient. Then, $\hat{Y}_p(t) = \tilde{Y}_p(t)$ is obtained and the feedback signal corresponds to $\tilde{Y}_p(t)$. In this case, the controller reacts only when the reference changes or the process disturbances $d(t)$ influence the controlled variable. The algorithm flow chart for the proposed control scheme is shown in Figure 4.

In the real case, there are model uncertainties, especially those related to the static nonlinearity in the Wiener model, since it is virtually impossible to know the exact values of the parameters a priori. Actually, the linear part of the PK/PD model is also affected by uncertainties, related to parameters variability and model inaccuracies. Taking into account these issues, the $i(t)$ signal is used both to compensate modelling uncertainties and to react to the disturbances induced by surgical stimuli. As shown in Figure 2, the $i(t)$ value is related to the error between $\tilde{Y}_p(t)$ (estimated propofol effect-site concentration using linear part of the model, $\tilde{P}_{prop}$) and $\hat{Y}_p(t)$ (propofol effect-site concentration obtained via average Hill function inversion based on the real BIS measure). Thus, the GPC

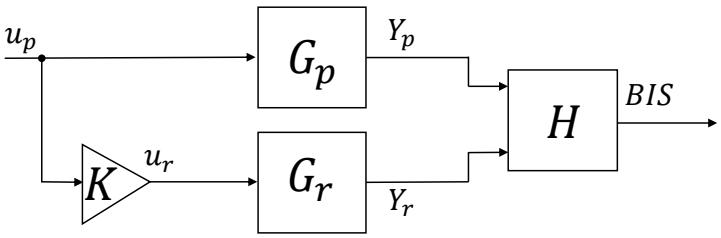

Fig. 3: Simplified scheme for the external predictor.

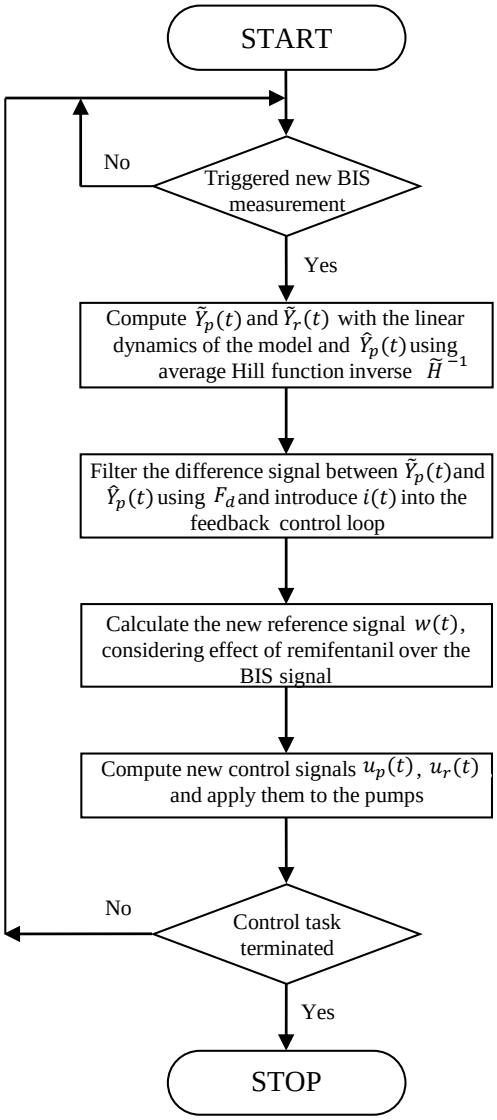

Fig. 4: Algorithm flow chart for developed control scheme.

controller uses $\check{Y}_p(t)$ as a feedback signal, which contains information regarding patient model mismatches and influence of disturbances.

In the same way, the proposed control system handles the patient's state changes along the time, which result in model inaccuracies. These could be related to a sudden change in patient's hemodynamics (which affects drugs clearances) that can be due to a severe blood loss or to the administration of vasoactive medications. As a consequence, the variation of the model parameters are considered as unmeasurable disturbances that needs to be compensated by the controller among other modelling errors.

Moreover, the $i(t)$ signal passes through the low-pass filter F_d. The main purpose of F_d is to attenuate the result of disturbances and uncertainties on the GPC feedback controller and, at the same time, to guarantee a null steady-state reference tracking error in the feedback loop.

The F_d filter is represented as a first order transfer function of the following form:

$$F_d(s) = \frac{1}{T_d s + 1} \tag{11}$$

where T_d is a time constant that needs to be adjusted. Therefore, to obtain the satisfactory performance of the control system, it is required to tune the GPC controller parameters as well as T_d. The detailed information regarding the control system tuning is in Section 3.4

It is worth stressing again that $\tilde{P}_{prop}$, $\tilde{P}_{remif}$ are computed using demographic parameters that result in an individualized controller. On the contrary, $\tilde{H}$ and $\tilde{H}^{-1}$ are obtained using average values for the population that can be found in the literature [53, 54]. These values are $E_{max} = 87.5$, $C_{e50,p}$ =4.92 μg/ml, $C_{e50,r}$ = 12.5 ng/ml, γ=2.69, β=1.5. The parameter E_0 can be measured and the precise individualized value can be provided for each patient before the induction phase (it is the BIS measure obtained for patient in the fully awake state).

3.3. Generalized Predictive Controller algorithm

As it is well known [55], GPC consists of applying a control sequence that minimizes a multistage cost function of the form:

$$J = \sum_{j=N_1}^{N} [\hat{y}(t+j|t) - w(t+j)]^2 + \sum_{j=1}^{N_u} \lambda [\Delta u(t+j-1)]^2 \tag{12}$$

where $\hat{y}(k+j|t)$ is an optimal system output prediction sequence performed with data known up to discrete time t, $\Delta u(t+j-1)$ is a future control increment sequence obtained from the cost function minimization with $\Delta = (1-z^{-1})$, N_1 and N are the minimum and maximum prediction horizons respectively, N_u is the control horizon and λ is weighing factor for the future control signal. The desired control performance is obtained through the selection of appropriate values for horizons and weighting factor (the tuning procedure is shown in Section 3.4). The reference signal is represented by $w(k+j)$ along the prediction horizon [55]. As highlighted previously, the $w(t)$ signal is calculated at every sampling period, with a receding horizon strategy and considering the interaction of the remifentanil over the propofol. In (12), the j-step ahead prediction of the system output with data up to time t (that is, $\hat{y}(k+j|t)$), is computed by means of the following model [55]:

$$A(z^{-1})\tilde{y}(t) = B(z^{-1})u(t-1) + \frac{e(t)}{\Delta} \tag{13}$$

where A and B are polynomials in discrete time using the backward shift operator z^{-1}. The $e(t)$ term is related to the white noise and is set to zero. The future process output predictions can be expressed using vectorial form as follows:

$$\widehat{\mathbf{y}} = \mathbf{G}\mathbf{u} + \mathbf{f} \tag{14}$$

where $\widehat{\mathbf{y}}$ refers to the vector of the future prediction of the process outputs, $\mathbf{G}$ is the matrix representing the process dynamics, $\mathbf{u}$ is the vector of future control signal values and $\mathbf{f}$ is the free response of the process (for more details see [55]).

3.3.1. Process constraints handling

The GPC algorithm is able to handle a variety of process constraints, ranging from those representing hardware limitations like actuator saturation and slew rates to those that allow a specific behavior of the controlled variable to be obtained, namely, process output constraints. However, to obtain the desired performance in the proposed control system, only those related to the infusion pumps are necessary. Given the limitations of the actuators, the constraints of the control signal (given as $u_{min} = 0$ mg/s and $u_{max} = 6.67$ mg/s for propofol) have to be handled during the control signal computation through the optimization procedure. The pump saturation limits $u_{min} \leq u(t) \leq u_{max}$ can be included as a set of inequalities imposed on the future control signal increments:

$$\mathbf{l}u_{min} \leq \mathbf{T}\Delta\mathbf{u} + u(t-1) \leq \mathbf{l}u_{max}.$$

where $\mathbf{T}$ is a lower triangular matrix of ones with $N \times N$ size and $\mathbf{l}$ is a vector of ones $(1 \times N)$. Due to the ratio approach with a fixed gain $K = 2$, the constraints for remifentanil are $u_{min} = 0$ μg/s and $u_{max} = 13.34$ μg/s.

The slew-rate constraints can be taken into account using a set of inequalities $\Delta u_{min} \leqslant u(t) - u(t-1) \leqslant \Delta u_{max}$ and considered on the control signal increments vector Δu. Using the vectorial form, they can be rewritten as:

$$\mathbf{l}\Delta u_{min} \leqslant \Delta\mathbf{u} \leqslant \mathbf{l}\Delta u_{max}$$

In this case the limitations of infusion pump related to slew-rate constraints are set to $-0.2 \leqslant \Delta\mathbf{u} \leqslant 0.2$ mg/s for propofol and, as a consequence, to $-0.4 \leqslant \Delta\mathbf{u} \leqslant 0.4$ μg/s for remifentanil.

Note that the constraints on the manipulated variable (the propofol infusion) are considered in the optimization procedure, while the constraints for the remifentanil are applied in accordance with the values obtained for propofol by taking into account the ratio gain K.

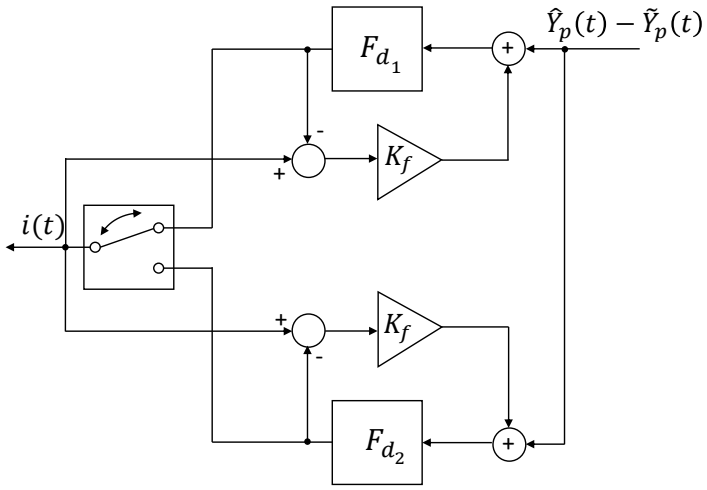

Fig. 5: The F_d block implementation details.

In general, the defined constraints can be expressed as $\mathbf{R}\Delta\mathbf{u} \leqslant \mathbf{c}$, where:

$$\mathbf{R} = \begin{bmatrix} \mathbf{I}_{N\times N} \\ -\mathbf{I}_{N\times N} \\ \mathbf{T} \\ -\mathbf{T} \end{bmatrix}; \mathbf{c} = \begin{bmatrix} \mathbf{l}\Delta u_{min} \\ -\mathbf{l}\Delta u_{max} \\ \mathbf{l}u_{max} - \mathbf{l}u(t-1) \\ -\mathbf{l}u_{min} + \mathbf{l}u(t-1) \end{bmatrix}.$$

where $\mathbf{I}_{N\times N}$ is the identity matrix (with $N \times N$ size). Lastly, all formulated constraints are handled in the QP optimization procedure, which is stated as:

$$J(\mathbf{u}) = \frac{1}{2}\mathbf{u}^T\mathbf{H}\mathbf{u} + \mathbf{b}^T\mathbf{u} + \mathbf{f}_0$$

subject to:

$$\mathbf{R}\Delta\mathbf{u} \leqslant \mathbf{c}$$

where $\mathbf{H} = 2(\mathbf{G}^T\mathbf{G} + \lambda\mathbf{I})$, $\mathbf{b}^T = 2(\mathbf{f} - \mathbf{w})^T\mathbf{G}$, $\mathbf{f}_0 = (\mathbf{f} - \mathbf{w})^T(\mathbf{f} - \mathbf{w})$ and $\mathbf{w}$ is the vector of the reference signal [55].

3.4. Control scheme parameters tuning

The controller parameters (N, N_u, and λ related to the GPC algorithm and T_d for the low-pass filter F_d) need to be selected in order to provide the desired performance and to assure the required robustness. It has been decided to tune the parameters for the set-point following and disturbance rejection tasks (namely, for the induction and maintenance phases) separately in a two steps approach [56–59]. In the first step of tuning procedure, the controller is setup to provide an optimal set-point tracking response. During second step, an additional tuning process is performed by keeping the values N and N_u obtained in the previous step and looking for λ and T_d values being optimized for disturbance rejection task. Thus, there are two sets of parameters; one is applied in the induction phase and the other one in the maintenance phase. In order to apply a bumpless switching for T_d, it is necessary to implement two different low-pass filters in the scheme, see Figure 5. When the filter of the induction phase is operating, the other one, for the maintenance phase, is in tracking mode assuring that its output is changed to be the same as $i(t)$ at the switching time instant.

By following the same approach used in [10,40,60], the tuning is performed using an optimization technique, in order to minimize the worst-case IAE (Integrated Absolute Error) taking into account the representative population of the 13 patients described in [10]. The optimization is performed by means of a genetic algorithm, where the initial population (of 40 elements) was generated using a uniform distribution provided by the a Gaussian mutation function. Being the IAE defined as:

$$IAE = \int |r(t) - BIS(t)|dt \tag{15}$$

finally, the objective function that minimizes the worst-case IAE is defined as:

$$\min_{N,N_u,\lambda,T_d} \max_{k\in\{1,\dots,13\}} IAE_k(N,N_u,\lambda,T_d), \tag{16}$$

where $IAE_k(N,N_u,\lambda,T_d)$ refers to the IAE value computed for the kth patient from the database. The resulting parameters for the induction phase (set-point following) are $N = 36$, $N_u = 34$, $\lambda = 10$ and $T_d = 96$. For the maintenance phase, the λ and the T_d values are changed respectively to 3 and 23.

4. Simulation results

In this section, the results obtained in simulation with the proposed control architecture are presented. Both induction and maintenance phases of anesthesia have been simulated, in order to verify the fulfilment of the clinical specifications and to assess the performance. The induction phase, which is a set-point following task, has been simulated providing to the controller a step reference signal, $r(t)$, that goes from the initial BIS value, E_0, to the target BIS value of 50. The maintenance phase is a disturbance rejection task where the BIS level of the patient is perturbed by the effect of the surgical stimulation. This has been simulated as an additive disturbance, $d(t)$, acting on patient's BIS. In particular, a double step disturbance signal has been applied. It consists of a positive step of amplitude 10 followed by a negative step of the same amplitude that brings the disturbance back to zero. This particular profile has been chosen since it is the most challenging one for a feedback controller. Moreover, the simulation results obtained with this disturbance profile can be easily interpreted and they are well representative of the disturbance rejection performance.
In order to evaluate the performance of the controller, the indexes proposed in [9] have been used. For the induction phase, the indexes are:

- TT: measured time-to-target for the BIS required to reach the target interval, $[45 \div 55]$, for the first time;
- BIS-NADIR: is the lowest value of BIS measure that is reached;
- ST10: is the settling time of the control system and it is calculated as the time period required for the BIS signal to get and continue within the interval of $[45 \div 55]$;
- ST20: the same of ST10, but it considers a BIS interval of $[40 \div 60]$;
- US: undershoot, defined as the difference between the BIS value of 45 and the BIS-NADIR.

For the maintenance phase, the indexes are:

- TTp: measured time-to-target necessary for bringing the BIS signal back into $[45 \div 55]$ interval after the positive step disturbance has occurred;
- TTn: measured time-to-target necessary for bringing the BIS signal back into $[45 \div 55]$ interval after the negative step disturbance occurred;
- BIS-NADIRp: the lowest observed BIS value after the positive step disturbance occurred and before the negative step disturbance occurred (undershoot);
- BIS-NADIRn: the highest observed BIS value after the negative step disturbance occurred (overshoot).

Initially, the controller performance has been assessed on the patient database of Table 1. Then, the robustness of the proposed control architecture has been analyzed by simulating the effect of intra- and inter-patient variability.

4.1. Test on a sample dataset

In this section, simulation results obtained on the patients dataset of Table 1 are presented. In this test, is assumed that the linear term of the considered process model is perfectly known ($\tilde{P}_{prop} = P_{prop}$ and $\tilde{P}_{remif} = P_{remif}$). However, the nonlinear element represented by the average Hill function is used instead of the actual patient's one ($\tilde{H} \neq H$). Figure 6 shows the control system performance for the induction and maintenance phases. The performance indexes related to the induction phase are shown in Table 2, while those of the maintenance phase are shown in Table 3. From the obtained results, it is possible to notice that the proposed control system provides a fast induction of anesthesia. Indeed, the mean TT over the whole dataset is 1.75 minutes, with a maximum value of 2.10 minutes obtained for patient 11. These values are fully compatible with the clinical specifications. The short TT has been achieved without causing an excessive undershoot of the BIS. In particular, BIS values below 50 have occurred in only two out of thirteen patients. Nevertheless, the BIS-NADIR has always remained above

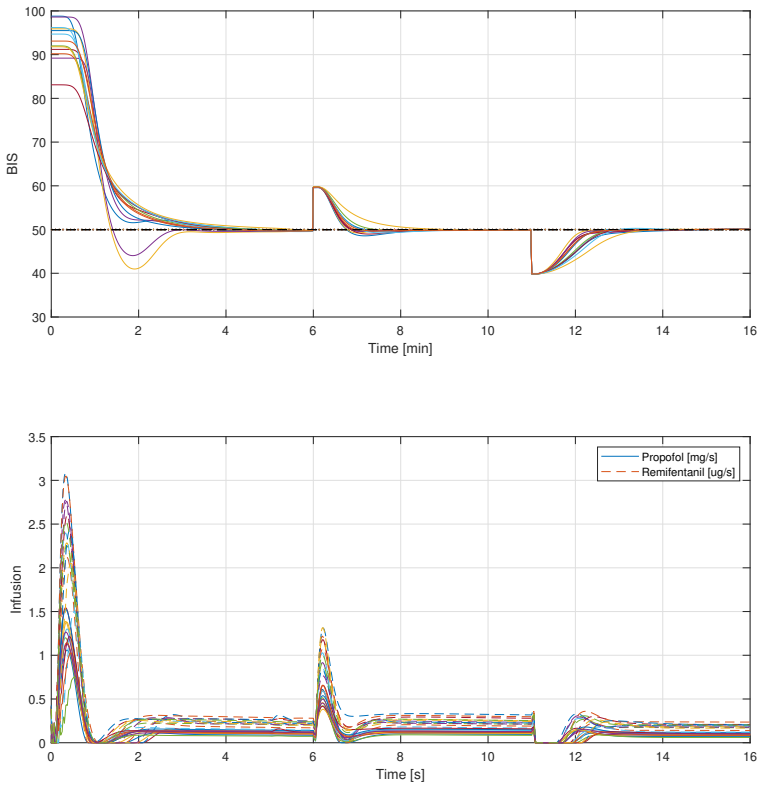

Fig. 6: Control system performance for induction and maintenance phases considering all the dataset patients.

Table 2: Induction phase - performance indexes for all patients.

Patient	TT [min]	BIS-NADIR	ST20 [min]	ST10 [min]	US
1	1.38	49.67	1.27	1.38	0.00
2	1.53	49.61	1.33	1.53	0.00
3	1.87	49.65	1.38	1.87	0.00
4	1.27	40.98	1.18	2.42	4.02
5	2.02	49.71	1.42	2.02	0.00
6	1.78	49.56	1.40	1.78	0.00
7	1.92	49.74	1.45	1.92	0.00
8	1.65	49.61	1.38	1.65	0.00
9	1.30	44.04	1.20	2.10	0.96
10	2.02	49.57	1.43	2.02	0.00
11	2.10	49.79	1.52	2.10	0.00
12	2.03	49.53	1.45	2.03	0.00
13	1.83	49.62	1.43	1.83	0.00
mean	1.75	48.54	1.37	1.89	0.38
std.dev	0.29	2.75	0.11	0.27	1.12
max	2.10	49.79	1.52	2.42	4.02
min	1.27	40.98	1.17	1.38	0.00

the recommended value of 40, and the undershoot has been short-lasting, as it appears from the values of ST10 and ST20. Indeed, ST20 is always shorter than TT. This indicates that the BIS quickly settles inside the recommended range 40-60. As regards the ST10, it is equal to TT for all the patients, except in the two patients for which an undershoot occurs. In any case, the maximum value is 2.42 minutes, hence the BIS always settles in the range 45-55 in less than 3 minutes. As regards the maintenance phase, the control system quickly compensates for the positive step disturbance as indicated by the TTp, without causing undershoot as the BIS-NADIRp never drops below 48. The TTn is longer than the TTp because the compensation of the negative step disturbance is mainly dominated by the patient natural dynamics. Indeed, when the negative step disturbance occurs, the controller reacts by decreasing the drugs flows until they saturate to zero. Anyway, the controller behaviour is sensible and the negative disturbance is compensated without causing a BIS overshoot, as it appears from the BIS-NADIRn index.

4.2. Test on a sample dataset subject to intra-patient variability

The robustness of the proposed control system has been assessed in the case of intra-patient variability. For this, a mismatch has been introduced also in the linear term of the analyzed process model. To this end, each of the thirteen patients of the considered dataset, $\tilde{P}_{prop}$ and $\tilde{P}_{remif}$ are calculated with the average parameters values, while a set of 500 perturbed P_{prop} and P_{remif} models is generated by a Monte Carlo Method (MCM) based on the statistical properties of the PK models given in [17] and [43]. For each of these perturbed models, the induction and maintenance phases have been simulated. As regards the induction phase, the results for the average patient are shown in Figure 7 and the corresponding performance indexes are given in Table 4. The defined clinical requirements are always fulfilled. The same behaviour has been obtained for all the other patients of the dataset and the corresponding results are shown in Figure 8. As regards the maintenance phase, the results for the average patient are shown in Figure 9 and the corresponding performance indexes are given in Table 5. Even in this scenario, the clinical requirements are always met. Moreover, the same behaviour has been obtained for all the other patients of the dataset and the results obtained are shown in Figure 10.

4.3. Test on a wide population

In order to assess further the robustness of the proposed control architecture, a random population of 500 patients has been generated again with a MCM. The population has been generated by selecting randomly the gender, and by employing a uniform distribution of the parameters. For the analyzed scenario, we select the ranges for age between 18 and 70, weight between 50 kg and 100 kg and height between 150 cm and 190 cm. The parameters of the nonlinear interaction model have been generated considering the statistical distribution given in [41,49,53]. In this context, it is assumed that the linear term of the considered process model is known ($\tilde{P}_{prop} = P_{prop}$ and $\tilde{P}_{remif} = P_{remif}$). On the contrary, the nonlinear element is represented by the average Hill function, that is implemented in the control scheme ($\tilde{H} \neq H$). The responses of the induction phase are shown in Figure 11 and the obtained performance indexes are given in Table 6.

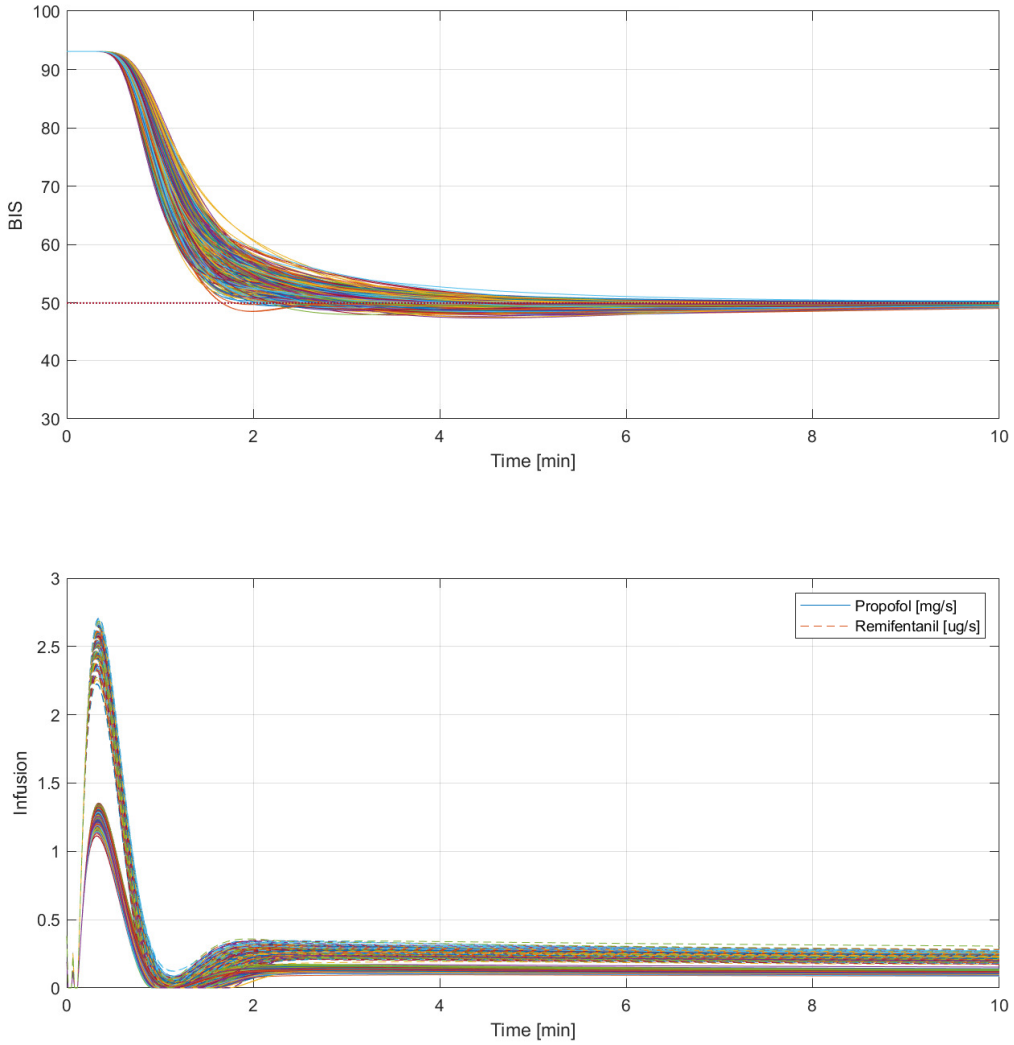

Fig. 7: Induction phase subject to intra-patient variability - MCM simulation results for the average patient.

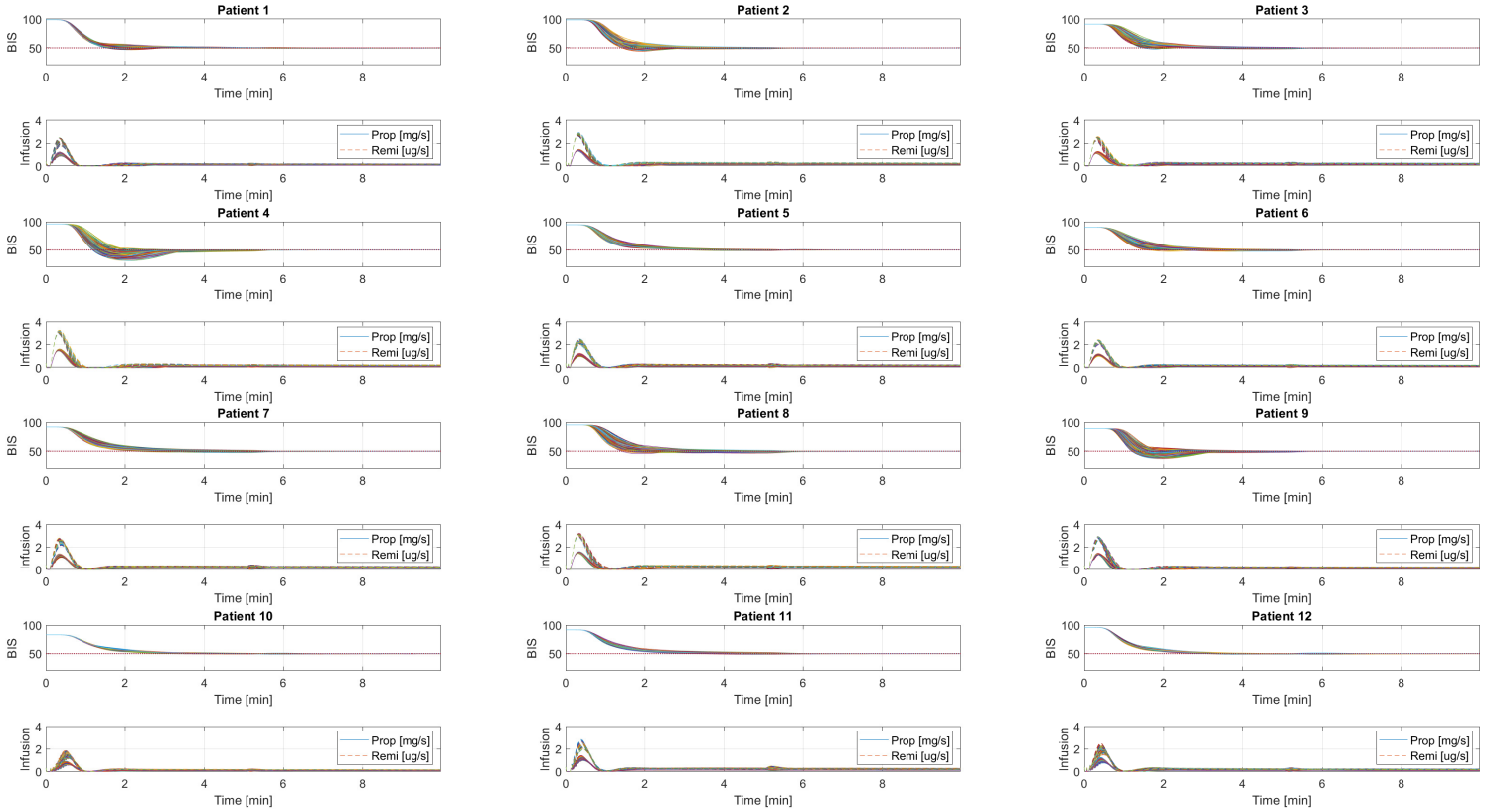

Fig. 8: Induction phase subject to intra-patient variability - simulation results for all the patients of the dataset.

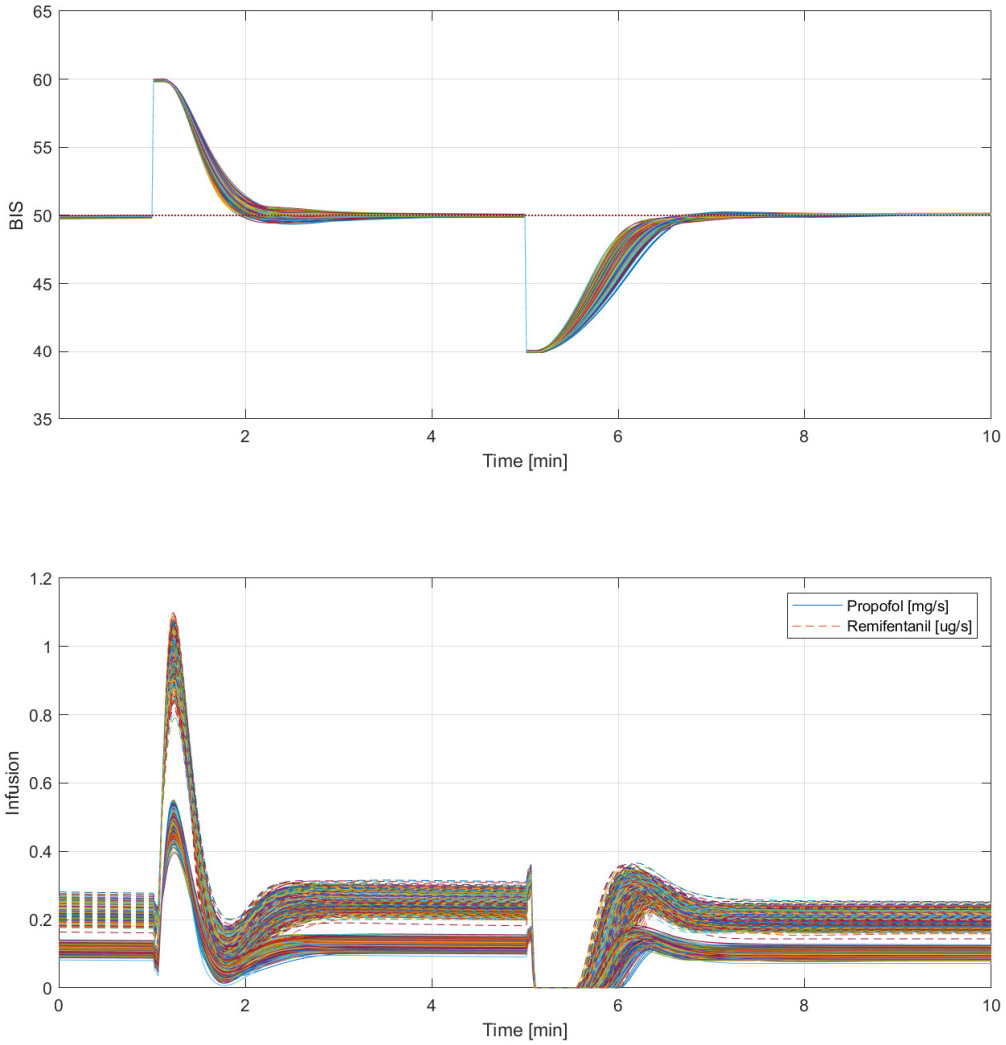

Fig. 9: Maintenance phase subject to intra-patient variability - MCM simulation results for the average patient.

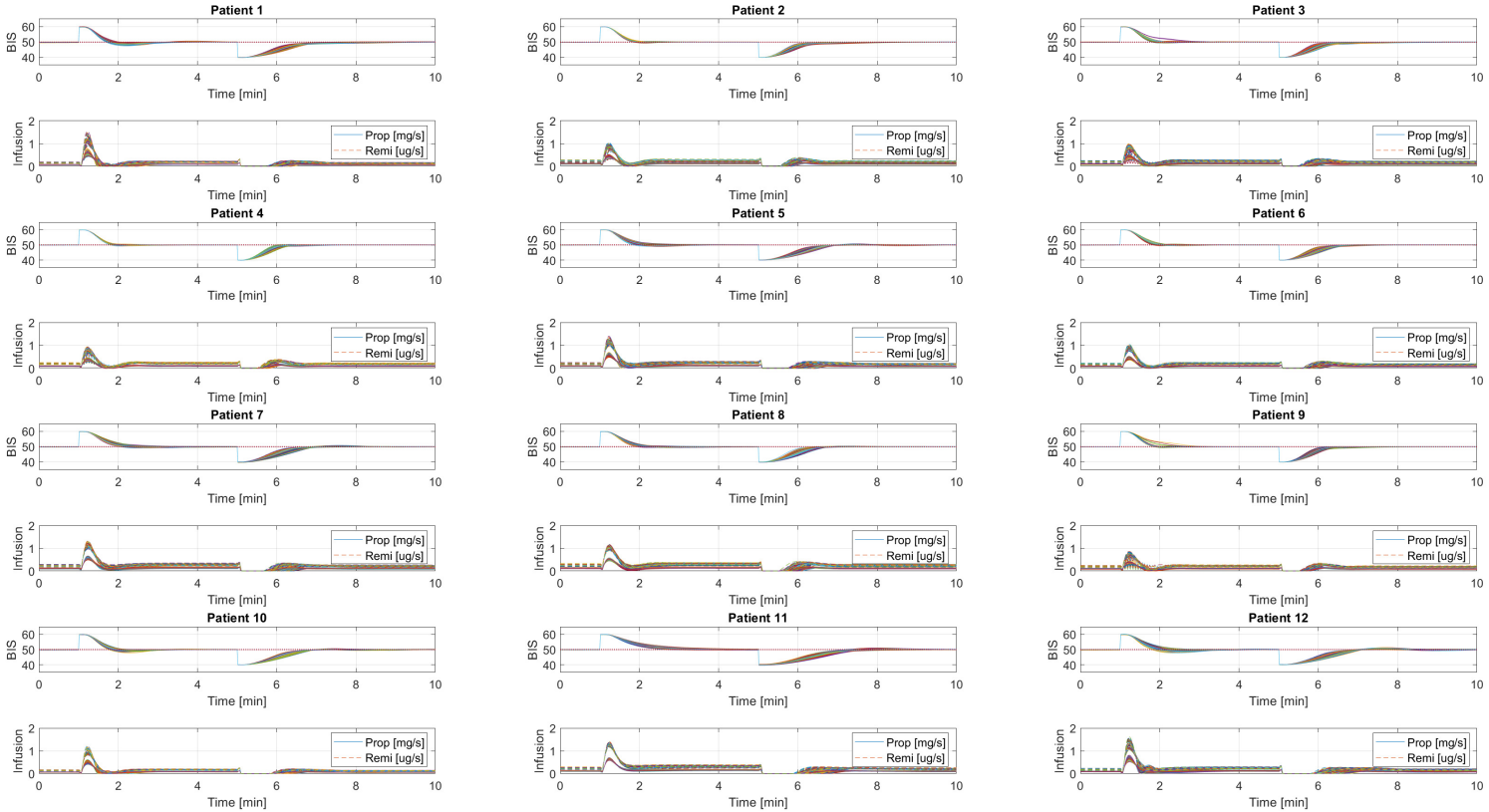

Fig. 10: Maintenance phase subject to intra-patient variability - simulation results for all the patients of the dataset.

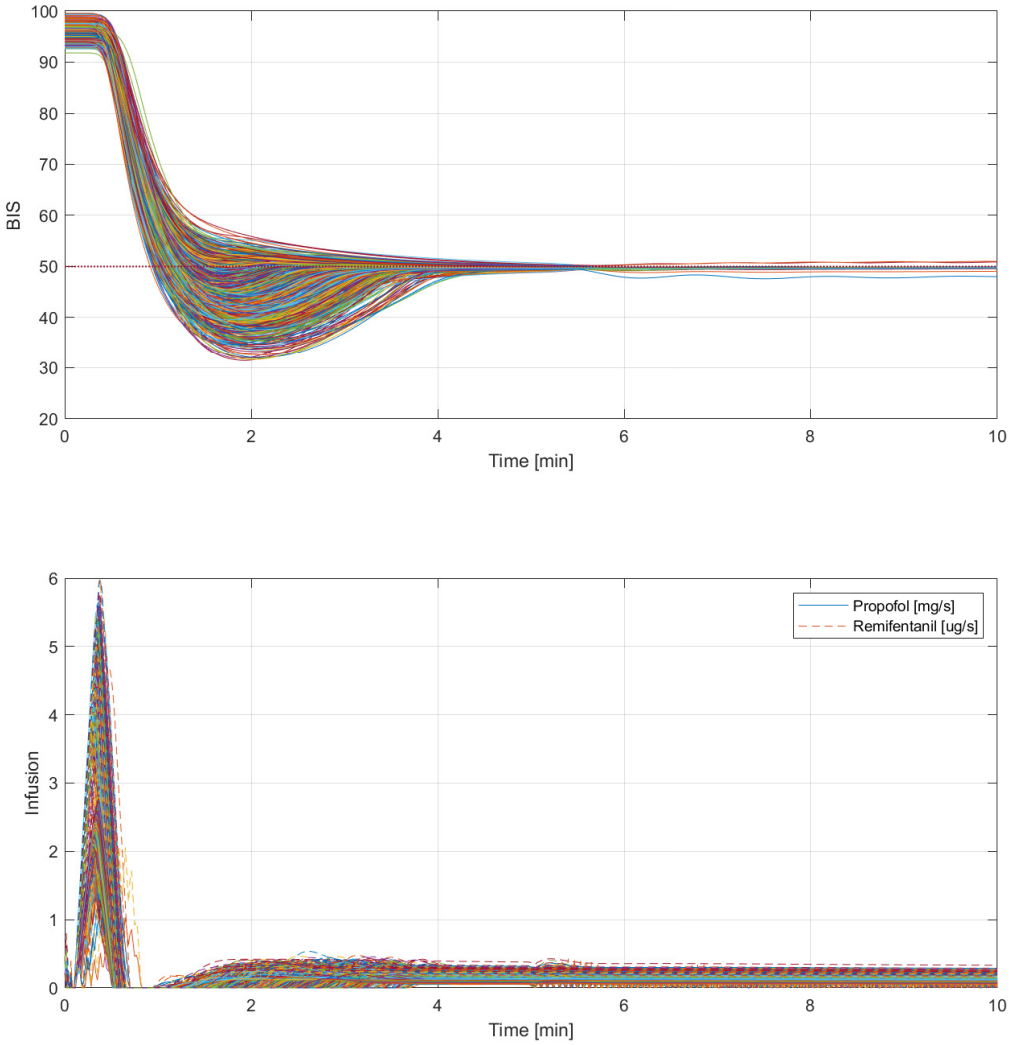

Fig. 11: Induction phase - MCM simulation results for the inter-patient variability.

Table 3: Maintenance phase - performance indexes for all patients.

	TTp [min]	BIS-NADIRp	TTn [min]	BIS-NADIRn
1	0.47	48.56	1.05	50.08
2	0.48	49.63	0.80	50.08
3	0.48	49.72	0.78	50.09
4	0.47	49.23	0.72	50.02
5	0.55	49.64	1.02	50.09
6	0.52	49.60	0.83	50.06
7	0.58	49.77	1.00	50.06
8	0.55	49.69	0.88	50.03
9	0.48	49.57	0.78	50.04
10	0.50	48.97	1.05	50.08
11	0.73	49.85	1.32	50.06
12	0.53	49.24	1.13	50.28
13	0.53	49.69	0.85	50.06
mean	0.53	49.47	0.94	50.08
std.dev	0.07	0.37	0.17	0.06
max	0.73	49.85	1.32	50.28
min	0.47	48.56	0.72	50.02

Table 4: Induction phase subject to intra-patient variability - performance indexes for the average patient with MCM evaluation.

	TT [min]	BIS-NADIR	ST20 [min]	ST10 [min]	US
mean	1.91	49.40	1.46	1.91	0.00
std.dev	0.24	0.40	0.13	0.24	0.00
min	1.37	47.89	1.13	1.37	0.00
max	2.67	49.86	1.93	2.67	0.00

The controller quickly induces anesthesia in all patients. Indeed, the mean TT is 1.13 minutes and its maximum value is 2.23 minutes. Thus, the clinical requirements are fully satisfied. As regards the BIS-NADIR, the mean value of 44.23 implies that the control system does not cause an excessive undershoot of the BIS. In some patients the BIS falls below the recommended threshold of 40, as it is possible to notice by observing the minimum value of the BIS-NADIR, which is 31.46. However, the undershoot values obtained are acceptable as BIS values up to 30 are commonly reached in clinical practice and are not harmful to the patient health. The ST20 and ST10 values are, also in this case, fully compatible with the clinical practice. With respect to the test on the dataset of thirteen patients, it is possible to observe an increase in their maximum values that is due to the more pronounced undershoot observed in some patients of the population. However, these values remain well below the recommended value of 5 minutes given in the clinical requirements. Figure 12 shows the responses obtained in the maintenance phase and the performance indexes corresponding to this scenario are given in Table 7. The results on the whole population confirmed those obtained on the dataset of thirteen patients. Indeed, the control system is able to reject the disturbances quickly without causing undershoot or overshoot of the BIS.

It should be highlighted that the proposed control system based on the constant ratio between the two drugs is one of approaches that could be exploited in clinical practice. For instance, it will be also interesting to develop a control system that will allow the anaesthesiologist to use a mix between manual and automatic control for multi drug infusion system. Such a hybrid system architecture will be addressed in our future works.

5. Conclusions

In this paper, a model predictive control strategy using a MISO approach for the anaesthesia process has been presented. The proposed control structure is based on the individualized multi-variable Wiener model, which is also used to decouple the drugs interactions effect for control purposes. The designed controller also takes advantage of the constraints handling mechanism, considering saturation and slew rates limitations on the computed control signals. The optimal control system parameters adjustment has been performed by means of genetic algorithms, taking into account a database of patients that is representative of a wide population. Moreover, the proposed con-

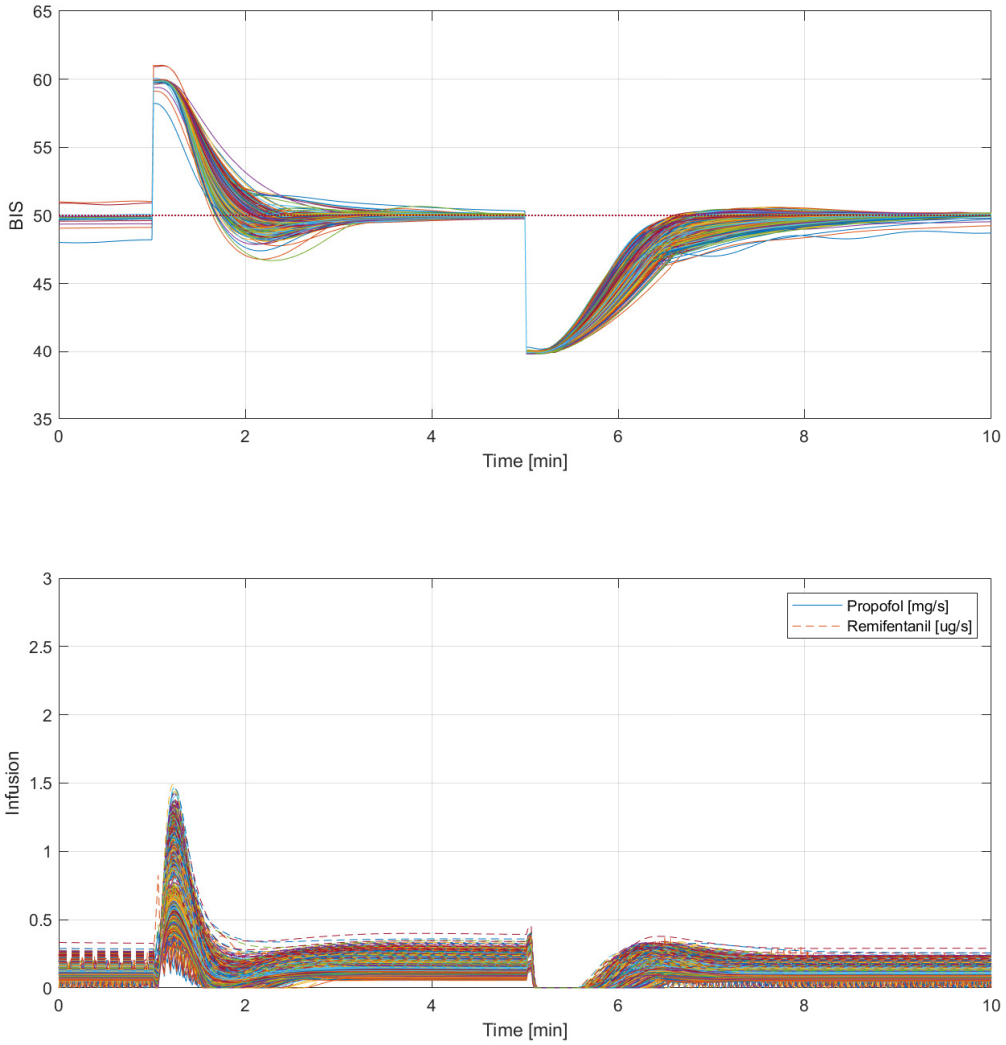

Fig. 12: Maintenance phase - MCM simulation results for the inter-patient variability.

Table 5: Maintenance phase subject to intra-patient variability - performance indexes for the average patient with MCM evaluation.

	TTp [min]	**BIS-NADIRp**	**TTn [min]**	**BIS-NADIRn**
mean	0.55	49.82	0.86	50.09
std.dev	0.02	0.08	0.06	0.03
min	0.50	49.36	0.68	50.03
max	0.62	49.95	1.05	50.27

Table 6: Induction phase - performance indexes with the MCM for inter-patient variability.

	TT [min]	**BIS-NADIR**	**ST20 [min]**	**ST10 [min]**	**US**
mean	1.13	44.23	1.27	1.95	2.23
std.dev	0.15	4.38	0.62	0.78	3.02
min	0.83	31.46	0.78	0.95	0.00
max	2.23	49.81	3.27	3.78	13.54

troller can be easily implemented and executed in real time on a standard PC. The effectiveness of the methodology has been demonstrated using an *in silico* approach exploiting the nonlinear patient model. Indeed, the obtained results have demonstrated that the proposed control structure gives a satisfactory performance despite inter- and intra-patient variability.

Future work will be oriented to provide practical evaluation of the developed controller under a real clinical conditions through an in vivo study. Moreover, it is planned to provide a hybrid control system architecture that enables the manual control of the remifentanil, providing optimal control of the propofol taking into account the synergistic relation between the drugs.

Acknowledgment

This work has been supported by EU–H2020 funds under MSCA Individual Fellowship - ACTAN project ID: 837912.
Authors would like to thank Paolo Visieri for his help with control system simulations and performance indexes computation.

References

1. C. Ionescu, M. Neckebroek, M. Ghita, D. Copot, An open source patient simulator for design and evaluation of computer based multiple drug dosing control for anesthetic and hemodynamic variables, IEEE Access 9 (2021) 8680–8694.
2. D. Copot, Automated Drug Delivery in Anesthesia, Academic Press, London, UK, 2020.
3. M. J. Khodaei, N. Candelino, A. Mehrvarz, N. Jalili, Physiological closed-loop control (PCLC) systems: Review of a modern frontier in automation, IEEE Access 8 (2020) 23965–24005.
4. M. Ghita, M. Neckebroek, C. Muresan, D. Copot, Closed-loop control of anesthesia: Survey on actual trends, challenges and perspectives, IEEE Access 8 (2020) 206264–206279.
5. E. Brogi, S. Cyr, R. Kazan, F. Giunta, T. M. Hemmerling, Clinical performance and safety of closed-loop systems: A systematic review and meta-analysis of randomized controlled trials, Anesthesia-Analgesia 124 (2) (2017) 446–455.
6. T. Mendonça, J. Lemos, H. Magalhães, P. Rocha, S. Esteves, Drug delivery for neuromuscular blockade with supervised multimodel adaptive control, IEEE Transactions on Control System Technology 17 (6) (2009) 1237–1244.
7. B. Andrade-Costa, M. Silva, T. Mendonça, J. Lemos, Neuromuscular blockade nonlinear model identification, Proceedings 17th Mediterranean Conference on Control & Automation, Thessaloniki, Greece, 2009.
8. M. Silva, T. Wigren, T. Mendonça, Nonlinear identification of a minimal neuromuscular blockade model in anaesthesia, IEEE Transactions on Control System Technology 20 (1) (2011) 181–188.
9. C. Ionescu, R. D. Keyser, B. Torrico, T. D. Smet, M. Struys, J. Normey-Rico, Robust predictive control strategy applied for propofol dosing using BIS as a controlled variable during anesthesia, IEEE Transactions on Biomedical Engineering 55 (9) (2008) 2161–2170.
10. L. Merigo, F. Padula, A. Pawlowski, S. Dormido, J. L. Guzman, N. Latronico, M. Paltenghi, A. Visioli, A model-based control scheme for depth of hypnosis in anesthesia, Biomedical Signal Processing and Control 42 (2018) 216–229.
11. J. M. Gonzalez-Cava, F. B. Carlson, O. Troeng, A. Cervin, K. van Heusden, G. A. Dumont, K. Soltesz, Robust PID control of propofol anaesthesia: Uncertainty limits performance, not PID structure, Computer Methods and Programs in Biomedicine 198 (105783) (2021) 1–8.

Table 7: Maintenance phase - performance indexes with the MCM for inter-patient variability.

	TTp [min]	BIS-NADIRp	TTn [min]	BIS-NADIRn
mean	0.53	49.38	1.03	50.14
std.dev	0.04	0.33	0.09	0.09
min	0.35	46.69	0.82	49.83
max	0.75	49.95	1.40	50.61

12. C. M. Ionescu, I. Nascu, R. D. Keyser, Towards a multivariable model for controlling the depth of anaesthesia using propofol and remifentanil, Proceedings of 8th IFAC Symposium on Biological and Medical Systems, Budapest, Hungary, 2012.
13. E. Furutani, K. Tsuruoka, S. Kusudo, G. Shirakami, K. Fukuda, A hypnosis and analgesia control system using a model predictive controller in total intravenous anesthesia during day-case surgery, Proceedings of SICE Annual Conference 2010, Taipei, Taiwan, 2010.
14. N. Cardoso, J. M. Lemos, Model Predictive Control of Depth of Anaesthesia: Guidelines for controller configuration, Proceedings of 30th Annual International Conference IEEE EMBS 2008, Vancouver, Canada, 2008.
15. M. Mahfouf, C. S. Nunes, D. A. Linkens, J. E. Peacock, Modelling and multivariable control in anaesthesia using neural-fuzzy paradigms part ii. closed-loop control of simultaneous administration of propofol and remifentanil, Artificial Intelligence in Medicine 35 (3) (2005) 207–213.
16. T. Bouillon, J. Bruhn, L. Radulescu, E. Bertaccini, S. Park, T. Shafer, Non-steady state analysis of the pharmacokinetic interaction between propofol and remifentanil, Anesthesiology 97 (2002) 1350–1362.
17. C. Minto, T. Schnider, T. Egan, E. Youngs, H. Lemmens, P. Gambus, V. Billard, J. Hoke, K. Moore, D. Hermann, K. Muir, Influence of age and gender on the pharmacokinetics and pharmacodynamics of remifentanil, Anesthesiology 86 (1997) 10–23.
18. C. Minto, T. Schnider, T. Short, K. Gregg, A. Gentilini, S. Shafer, Response surface model for anesthetic drug interactions, Anesthesiology 92 (6) (2000) 1603–1616.
19. J. M. Gonzalez-Cava, J. A. Reboso, J. L. Calvo-Rolle, J. A. Mendez-Perez, Adaptive drug interaction model to predict depth of anesthesia in the operating room, Biomedical Signal Processing and Control 59 (101931) (2020) 1–9.
20. J. Silva, A. S. Noe, T. Mendonca, P. Rocha, Modelling and indentification for the action of propofol and remifentanil on the BIS level, IFAC-PapersOnLine 53 (2) (2020) 16197–16202.
21. G. A. Perez, J. A. Mendez-Perez, S. T. Álvarez, J. A. R. Morales, A. M. L. Fragoso, Modelling the PSI response in general anesthesia, Journal of Clinical Monitoring and Computing 35 (5) (2021) 1015–1025.
22. H. C. Lee, H. G. Ryu, E. J. Chung, C. W. Jung, Prediction of bispectral index during target-controlled infusion of propofol and remifentanil: a deep learning approach, Anesthesiology 128 (3) (2018) 492–501.
23. A. Savoca, K. van Heusden, D. Manca, J. M. Ansermino, G. A. Dumont, The effect of cardiac output on the pharmacokinetics and pharmacodynamics of propofol during closed-loop induction of anesthesia, Computer Methods and Programs in Biomedicine 192 (105406) (2020) 1–10.
24. K. van Heusden, J. M. Ansermino, G. A. Dumont, Robust miso control of propofol-remifentanil anesthesia guided by the neurosense monitor, IEEE Transactions on Control Systems Technology 26 (5) (2018) 1758–1770.
25. N. Liu, T. Chazot, S. Hamada, A. Landais, N. Boichut, C. Dussaussoy, B. Trillat, L. Beydon, E. Samain, D. I. Sessler, M. Fischler, Closed-loop coadministration of propofol and remifentanil guided by bispectral index: a randomized multicenter study, Anesthesia-Analgesia 112 (3) (2017) 546–557.
26. N. West, K. van Heusden, M. Görges, S. Brodie, A. Rollinson, C. L. Petersen, G. A. Dumont, J. M. Ansermino, R. N. Merchant, Design and evaluation of a closed-loop anesthesia system with robust control and safety system, Anesthesia-Analgesia 127 (4) (2018) 883–894.
27. L. Merigo, F. Padula, N. Latronico, M. Paltenghi, A. Visioli, Event-based control tuning of propofol and remifentanil coadministration for general anaesthesia, IET Control Theory and Applications 14 (19) (2020) 2995–3008.
28. M. Neckebroek, J. H. L. Boldingh, T. D. Smet, M. M. R. F. Struys, Influence of remifentanil on the control performance of the bispectral index controlled bayesian-based closed-loop system for propofol administration, Anesthesia-Analgesia 130 (6) (2020) 1661–1669.
29. L. Merigo, F. Padula, N. Latronico, M. Paltenghi, A. Visioli, Optimized PID control of propofol and remifentanil coadministration for general anesthesia, Communications in Nonlinear Science and Numerical Simulation 72 (2019) 194–212.
30. M. Schiavo, F. Padula, N. Latronico, L. Merigo, M. Paltenghi, A. Visioli, Performance evaluation of an optimized PID controller for propofol and remifentanil coadministration in general anesthesia, IFAC Journal of Systems and Control 15 (100121) (2021) 1–16.
31. F. N. Nogueira, T. Mendonca, P. Rocha, Positive state observer for the automatic control of the depth of anesthesia—clinical results, Computer Methods and Programs in Biomedicine 171 (2019) 99–108.
32. M. Hosseinzadeh, K. van Heusden, M. Yousefi, G. A. Dumont, E. Garone, Safety enforcement in closed-loop anesthesia—a comparison study, Control Engineering Practice 105 (104653) (2020) 1–10.

33. K. Soltesz, G. A. Dumont, K. van Heusden, T. Hägglund, J. M. Ansermino, Simulated mid-ranging control of propofol and remifentanil using EEG-measured hypnotic depth of anesthesia, Proceedings of 51st IEEE Conference on Decision and Control (CDC), 2012, Maui, USA, 2012.
34. C. M. Ionescu, R. D. Keyser, M. M. R. F. Struys, Evaluation of a propofol and remifentanil interaction model for predictive control of anesthesia induction, Proceedings of 50th IEEE Conference on Decision and Control and European Control Conference 2011, Orlando, USA, 2011.
35. N. Eskandari, K. van Heusden, G. A. Dumont, Extended habituating model predictive control of propofol and remifentanil anesthesia, Biomedical Signal Processing and Control 55 (101656) (2020) 1–6.
36. S. Hall, Real-time projected gradient based NMPC with an application to anesthesia control, Master Thesis, Swiss Federal Institute of Technology, Zurich, Switzerland, 2020.
37. S. Khosravi, Constrained Model Predictive Control of Hypnosis, PhD thesis at University of British Columbia, Vancouver, Canada, 2015.
38. Z. Cao, E. Dassau, R. Gondhalekar, F. Doyle, Extremum seeking control based zone adaptation for zone model predictive control in type 1 diabetes, IFAC-PapersOnLine 50 (1) (2017) 15074–15079.
39. Z. Cao, R. Gondhalekar, E. Dassau, F. Doyle, Extremum seeking control for personalized zone adaptation in model predictive control for type 1 diabetes, IEEE Transactions on Biomedical Engineering 65 (8) (2018) 1859–1870.
40. A. Pawlowski, M. Schiavo, N. Latronico, M. Paltenghi, A. Visioli, Linear MPC for anesthesia process with external predictor, Computers and Chemical Engineering 161 (107747) (2022) 1–13.
41. T. W. Bouillon, J. Bruhn, L. Radulescu, C. Andresen, T. J. Shafer, C. Cohane, S. L. Shafer, Pharmacodynamic interaction between propofol and remifentanil regarding hypnosis, tolerance of laryngoscopy, bispectral index, and electroencephalographic approximate entropy, Anesthesiology 100 (6) (2004) 1353–1372.
42. T. Koitabashi, J. Johansen, P. Sebel, Remifentanil dose/electroencephalogram bispectral response during combined propofol/regional anestesia, Anesthesia & Analgesia 94 (6) (2002) 1530–1533.
43. T. W. Schnider, C. F. Minto, P. L. Gambus, C. Andresen, D. B. Goodale, E. J. Youngs, The influence of method of administration and covariates on the pharmacokinetics of propofol in adult volunteers, Anesthesiology 88 (1998) 1170–1182.
44. T. W. Schinder, C. F. Minto, S. L. Shafer, P. L. Andersen, D. B. Goodale, E. J. Youngs, The influence of age on propofol paharmacodynamics, Anesthesiology 90 (1999) 1502–1516.
45. L. Merigo, M. Beschi, F. Padula, N. Latronico, M. Paltenghi, A. Visioli, Event based control of propofol and remifentanil coadministration during clinical anesthesia, Proceedings of the 3rd International Conference on Event-Based Control, Communication and Signal Processing (EBCCSP), 2017, Funchal, Portugal.
46. Z. Guo, A. Medvedev, L. Merigo, N. Latronico, M. Paltenghi, A. Visioli, Synthetic patient database of drug effect in general anesthesia for evaluation of estimation and control algorithms, Proceedings 18th IFAC symposium on system identification, Stockholm, Sweden, 2018.
47. I. Nascu, R. Oberdieck, E. N. Pistikopoulos, Explicit hybrid model predictive control strategies for intravenous anaesthesia, Computers and Chemical Engineering 106 (2017) 814–825.
48. M. Struys, T. D. Smet, S. Greenwald, A. Absalom, S. Binge, E. Mortier, Performance evaluation of two published closed-loop control systems using bispectral index monitoring: a simulation study, Anesthesiology 95 (1) (2004) 6–17.
49. S. Kern, G. Xie, J. White, T. Egen, A response surface analysis of propofol-remifentanil pharmacodynamic interaction in volunteers, Anesthesiology 100 (6) (2004) 1373–1381.
50. J. Bruhn, T. W. Bouillon, S. L. Shafer, Bispectral index (BIS) and burst suppression: revealing a part of the BIS algorithm, Journal of Clinical Monitoring and Computing 16 (8) (2000) 593–596.
51. M. Soehle, A. Dittmann, R. K. Ellerkmann, G. Baumgarten, C. Putensen, U. Guenther, Intraoperative burst suppression is associated with postoperative delirium following cardiac surgery: a prospective, observational study, BMC Anesthesiology 15 (1) (2015) 61.
52. J. Vuyk, M. J. Mertens, E. Olofsen, A. G. L. Burm, J. G. Bovill, Propofol anesthesia and rational opioid selection determination of optimal EC50-EC95 propofol-opioid concentrations that assure adequate anesthesia and a rapid return of consciousness, Anesthesiology 87 (6) (1997) 1549–1562.
53. A. Vanluchene, H. Vereecke, O. Thas, E. Mortier, S. Shafer, M. Struys, Spectral entropy as an electroencephalographic measure of anesthetic drug effect: a comparison with bispectral index and processed midlatency auditory evoked response, Anesthesiology 101 (2004) 34–42.
54. L. Merigo, Automatic Control Strategies for Optimized Drug Administration in Anesthesia, PhD theis, University of Brescia, Brescia (IT), 2015.
55. E. F. Camacho, C. Bordóns, Model Predictive Control, Springer-Verlag, London, UK, 2007.
56. A. Pawlowski, L. Merigo, J. L. Guzman, A. Visioli, S. Dormido, Event-based GPC for depth of hypnosis in anesthesia for efficient use of propofol, Proceedings of the 3rd International Conference on Event-Based Control, Communication and Signal Processing (EBCCSP), 2017, Funchal, Portugal.
57. A. Pawlowski, L. Merigo, J. Guzmán, S. Dormido, A. Visioli, Two-degree-of-freedom control scheme for depth of hypnosis in anesthesia, IFAC-PapersOnLine 51 (4) (2018) 72–77.
58. A. Pawlowski, J. L. Guzmán, M. Berenguel, F. G. Acién, Control system for pH in raceway photobioreactors based on Wiener models, IFAC-PapersOnLine 52 (1) (2019) 928–933.
59. A. Pawlowski, M. Schiavo, N. Latronico, M. Paltenghi, A. Visioli, MPC for Propofol Anesthesia: the Noise Issue,

Proceedings of 6th IEEE Conference on Control Technology and Applications – CCTA 2022, Trieste, Italy, 2022.
60. F. Padula, C. Ionescu, N. Latronico, M. Paltenghi, A. Visioli, G. Vivacqua, Optimized PID control of depth of hypnosis in anesthesia, Computer Methods and Programs in Biomedicine 144 (2017) 21–35.